The mesoscopic and microscopic structure of the Vangorda deposit, Anvil District, Yukon: A preliminary report.

Dennis Brown
Department of Geology
Royal Holloway and Bedford New College
University of London
Egham
Surrey, TW20 OEX
U.K.

For: Curragh Resources,
117 Industrial Rd.
Whitehorse, Yukon

May 20, 1991

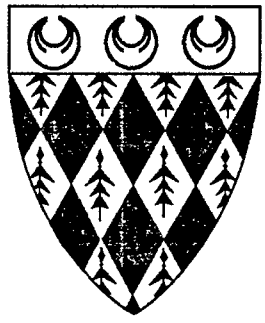

Introduction

The Vangorda Pb-Zn-Ag deposit forms a small, relatively shallow SEDEX-type massive sulphide ore body in the Anvil Mining District, Yukon, Canada. The ore body is polydeformed and likely displays structural elements related to all five phases of deformation reported in the Anvil District by Jennings and Jilson (1987).

The first phase of deformation in the area, D_1, is related to northeast-directed folding and thrusting during the pre- to mid-Cretaceous docking of outboard terranes. The only structural element found within the Vangorda deposit that can be unambiguously related to D_1 is a subvertical foliation (S_1) that is preserved as a lithon texture in the hinge areas of later folds. The second deformation event in the area is the regional D_2 deformation which is related to emplacement and unroofing of the Anvil Plutonic Suite during the Cretaceous (Jennings and Jilson 1987). D_2 structural elements found in the Vangorda deposit include macroscopic and mesoscopic southwest-verging F_2 folds and a southwest-dipping axial planar foliation (S_2). Also, several southwest-dipping faults occur in the deposit that are parallel to the S_2 axial surface, and along which there appears to have been significant offset (eg. Main Zone Fault, section 22+00E)(Brown 1990). These faults may in fact be D_2 thrusts. The effect of the regional D_3 to D_5 deformation events on the Vangorda deposit is largely unknown. In pit exposures, F_2 folds are locally refolded and there is a locally developed foliation. However, these features are of minor importance.

Extensional faults, related to unroofing of the Anvil Plutonic Suite, truncate all earlier structural features both within the Anvil District as a whole, and in the Vangorda deposit.

To date, all metamorphic effects in the Vangorda deposit is thought to be due to contact metamorphism related to intrusion of the Anvil Plutonic Suite. Metamorphic grade, recorded by muscovite-chlorite assemblages in the wall rock phyllites, is sub-

to mid-greenschist facies.

This report looks at the mesoscopic structural features in drill core and hand specimen from the Vangorda ores to investigate the structural style and the relationships between various structural elements. As well, a petrographic examination of sulphide microtextures within certain units of the ore body have been carried out and specific examples of these will be described. In particular, the deformation textures developed in pyrite are looked at using both reflected light and scanning electron microscopy.

Lithostratigraphy

The Vangorda deposit ores are a part of the Anvil Cycle as defined by Jennings *et al.* (1980) and Jennings and Jilson (1987). These authors recognised a number of sulphide lithofacies in the Anvil Cycle that are common to all the deposits in the Anvil District. The salient features of each lithofacies given by Jennings and Jilson (1987) are outlined below, with specific reference to the Vangorda deposit.

Massive pyritic sulphides: these rocks are typically massive pyrite with lesser sphalerite, galena, and minor magnetite occurring in either discrete bands or coarse-grained aggregates. Quartz, barite, and carbonates are disseminated throughout or occur in aggregates.Total sulphide content varies from between 60% to close to 100%. Texturally the massive pyritic rocks are homogeneous to banded. Banding is developed on a scale of millimetres to centimetres as alternating thick bands of pyrite and thin bands of sphalerite + magnetite + galena. A foliation, defined by chlorite + carbon in common.. Both the banding and the foliation are locally folded.

Baritic, massive pyritic sulphides: these consist predominantly of barite with pyrite, sphalerite, galena, with minor magnetite. Quartz and carbonate are major matrix components. Clasts of pyrite and phyllite are common. Total barite content varies but may be has high as 50 %. Millimetre- to centimetre-scale interbanding of

pyrite-rich and barite-rich layers is ubiquitous. Banding is often folded.

Pyrrhotitic massive sulphides: contains predominantly pyrrhotite with lesser pyrite, sphalerite, galena, and chalcopyrite. These rocks are typically highly brecciated, and contain clasts of other lithofacies. Clasts are rounded to angular, and generally have an internal foliation. Clasts may have symmetric or asymmetric tails indicating flattening or rotation, respectively, and rolling structures are common. The internal foliation in clasts is usually at an angle to the external foliation.

Pyritic quartzite: consists predominantly of quartz with up to 40% pyrite and minor sphalerite and galena. These rocks are moderately to poorly banded with, locally, a well developed micaceous foliation. Commonly the pyritic quartzites display a 'mottled' texture in which sulphides and quartz occur in discontinuous, random, shapeless segregations. Folding of the banding is common.

Sphalerite-rich quartzite: this rock type is a variant of the pyritic quartzite in which the dominant sulphide is sphalerite with lesser galena. Coarse patches of sphalerite or galena are common. Pyrite is rare and typically occurs as submillimetre-sized porphyroblasts or in isolated clasts. These rocks are typically highly brecciated and contain clasts of other rock types around which a well developed foliation anastomoses. As in the pyrrhotitic breccias, tailed clasts and rolling structures are common.

Ribboned-banded, carbonaceous, pyritic quartzite: these rocks are well banded, sulphide-bearing quartzite, with lesser sphalerite and galena. Bands are on a millimetre- to centimetre-scale and consist of quartz-sulphide bands and carbonaceous, phyllitic quartzite. Folding is typically found in these rocks, and preservation of banding in lithons is common.

Structure

This section looks at the mesoscopic structural elements developed in the ore rocks of the Vangorda deposit. The structural framework established for the Anvil District by Jennings and Jilson (1987) is followed in this report.

Folds

All rocks in the deposit have been penetratively deformed by the D_1 and D_2 deformation events, making definition of any primary depositional features on a mesoscopic scale ambiquous at best. In most rock types in the deposit, banding is well developed on a scale of millimetres to centimetres (see above). This banding is commonly folded by south- to southwest-verging folds accepted to be F_2. This banding is therefore taken to be a D_1 feature (i.e. S_1). Throughout the deposit S_1 is commonly preserved as lithons in the hinges of F_2 folds (Fig. 1). In F_2 fold limbs, however, S_1 has been transposed into subparallelism with the F_2 axial surface. S_1 is used throughout this report as the datum marker for referencing relative ages of structural elements.

Positive identification of F_1 folds in Vangorda rocks has not been made previously due to penetrative overprinting by F_2. However, the ubiquitous presence of S_1 in, and the evidence for F_1 folding in rocks in close proximity to the deposit (eg. Jennings and Jilson 1987), suggest that F_1 folding likely plays an important role in the present geometry of the deposit.

The dominant fold phase in the Vangorda deposit is F_2, and together with extensional faults provide the major structural control on the present geometry of the ore body. Mesoscopic F_2 folds are tight to isoclinal (interlimb angle is commonly between 5 to 25 degrees) similiar folds (Fig. 2). F_2 fold morphology

changes somewhat between different lithofacies as a result of relative competency and ductility contrasts between them, but in general the similiar style is maintained. In areas where the competency contrast is high F_2 folds become disharmonic.

In some lithofacies, a differentiated axial planar S_2 foliation, defined by aligned micas and carbon, is well developed in F_2 hinge zones. S_2 appears to be non-penetrative, and in the more sulphide-rich lithofacies is generally not found. In the latter situation, the S_1 banding is often transposed into subparallelism with the S_2 orientation, and may be easily mistaken for S_2.

Because of the problem of orientating fold axes relative to drill core axis, it is impossible to accurately determine fold plunge amounts and directions. However, fold axes were measured as a pitch in the S_2 foliation surface (assumed to dip shallowly southwest), which gives a qualitative estimate of fold orientations. Measured in this way, fold axes are generally subparallel to the strike of S_2 or have a small pitch angle in the S_2 surface. This is in agreement with F_2 fold orientations measured in the Vangorda open pit (Brown 1990).

There is, to date, very little evidence for the relationship between F_1 and F_2 folds in the Vangorda deposit, and it is assumed that the style of overprinting is the same as that recorded regionally (type 3) (cf Jennings and Jilson 1987, figure 21). In one example from the ribboned-banded quartzite lithofacies examined in this study, a quartz band in a phyllite matrix is folded by a tight F_2 fold (Fig. 3a). A differentiated axial plane cleavage dips ~ 110 ^{o} relative to the core axis. The quartz band appears to be continuous around a closure near the top of the sample suggesting it has been previously folded by an upright (relative to core axis) F_1 fold whose limbs and axial surface were subsequently overprinted by the F_2 fold (Fig. 3b). Also, along the edge of the core there are several small, tight folds with axial surfaces oriented subparallel to core axis, and at a high angle to S_2. These are also interpreted to be F_1. The geometry of the refold pattern outlined by these structures is type 3, similiar to the regional pattern.

On the scale looked at in this report the only post-D_2 structural elements recorded in the Vangorda deposit is a local foliation that clearly cross-cuts S_1 and S_2. It is not known which generation of structures these belong to, or in fact if they are all of the same generation.

Faults

A wide variety of faults occur throughout the deposit, and range in scale from millimetres to several meters in structural thickness. Faults in the deposit manifest themselves in two main ways; 1) brittle faults expressed as gouge or breccia zones, and 2) ductile shear zones. This report looks at faults only on the scale of one up to several centimetres. Because the samples used in this study are from unoriented drill core and hand specimens, kinematic indicators cannot be used to determine the geometry of the shear zone.

Brittle faults in the deposit are typically gouge zones consisting of phyllosilicates and/or sulphide-quartz sand. The unconsolidated nature of these gouge zones makes them very difficult to study and they are not discussed further. Locally, however, brittle faults are cemented by a matrix of quartz and calcite. These contain angular clasts of phyllite and sulphides ranging in size from several millimetres up to several centimetres (Fig. 4). Clasts are themselves strongly broken up and, in many cases, can be fitted back together. The presence of clasts of quartz matrix in the fault zone in figure 4 indicates several movement episodes occurred. In sulphide clasts, porphyroblasts of pyrite are common.

By far the most common fault in the ore rock samples looked at are ductile shear zones, known colloquially as ductile flow breccias (Fig. 5). Ductile flow breccias in these samples range in size from several millimetres up to several 10,s of centimetres wide. Their boundaries can be diffuse or, in many cases, very sharp. The characteristics of ductile flow breccias range from dominantly pyrrhotite or sphalerite matrix with small extremely rounded clasts, to dominantly angular to

rounded clasts with lesser martix.These shear zones exhibit durchbewegung structure (see Marshall and Gilligan 1989) in which there is tectonic mixing of angular to rounded clasts of brecciated quartz, phyllite, and sulphide in a ductilely deformed, well foliated, and recrystallized pyrrothite-rich or, often, sphalerite and galena-rich matrix (Fig. 5). Late (?) 'buckshot' porphyroblasts of pyrite are common in the matrix and in sulphide clasts. Clasts are commonly tailed or rotated, and in some cases are internally folded, with the foliation flowing around them.Thin ductile flow breccias are common along boundaries between sulphide lithofacies, suggesting layer parallel shearing was active during deformation. The sphalerite-rich faults are commonly very high grade ore rocks.

In one spectacular example of incipient durchbewegung structure (Fig. 6a), an isoclinally F_2 (?) folded band of fine-grained pyrite in a matrix of sphalerite, galena, and porphyroblastic pyrite displays an array of structures. For instance, in the hinge zone of the fold (Fig. 6b), the less competent matrix has pierced the pyrite band forming an equant piercement cusp. Also, along a limb, the pyrite band has under gone pinch and swell, and boudinage with the matrix flowing into boudin necks. As well, matrix material as intruded the pyrite band in a fashion similiar to piercement viens, causing it to brecciate (Fig. 6b). Further, tailed pyritic clasts show internal folding, indicating a sense of shear. Late fractures cross-cut the pyrite band, but in most cases does not extend into the matrix, a clear indication of the competency contrasts between them..

Another feature of interest in this sample is the partially resorbed nature of the edge of the pyrite band, which suggests reactions taking place between the pyrite-rich material and the matrix. Rusty-colored, discontinuous wisps of pyrite-rich matrix may represent near complete resorbtion of pyrite bands. This feature will be further looked at in the future.

Microstructure

This report looks at several microstructural aspects of ore rocks from the Vangorda deposit, but concentrates mainly on deformation textures in pyrite. Polished blocks for reflected light microscopy were prepared and from these selected samples were etched with nitric acid (HNO_3) to study growth features (eg. grain boundaries and overgrowths), different phases of each mineral, and deformation textures (eg. dislocation structures).

Optical microstructures

Examples of sphalerite microstructures are limited to those observed in the matrix of massive pyrite and pyritic quartzite lithofacies. In these samples, sphalerite typically forms a fine- to medium-grained mosaic of submillimetre-sized equant to xenoblastic grains in the interstices between larger porphyroblasts of pyrite. In some cases, equilibrium textures such as straight to mildly sutured grain boundaries with 120^{o} triple junctions are apparent. In other cases, grain boundaries are strongly curved to lobate, indicating grain boundary migration processes during annealing. Twinning in sphalerite is commonly broad annealing twins (Fig. 7), although thin, tapered deformation twins do occur. Locally, as in figure 7, sphalerite is exsolving to chalcopyrite.

One small grain of gold was found as an inclusion in pyrrhotite (Fig. 8)

So far his study has been based mainly on the textures shown by pyrite. Relict, primary colloform pyrite grains, although rare, still occur in the massive pyrite and pyritic quartzite lithofacies (Fig.9). These are typically equant to xenoblastic grains that occur alone or as cores in overgrowths of secondary, metamorphic pyrite.

Secondary, metamorphic pyrite, identifiable by its massive, typically inclusion-poor, equant to idioblastic nature, show a number of annealing textures due to metamorphism. For instance, in the massive pyritic lithofacies, grains are commonly submillimetre- to millimetre-sized, equant grains with straight to mildly sutured grain boundaries that meet at 120^{o} triple junctions. Also, in more quartz-rich areas and in the pyritic quartzite lithofacies, pyrite commonly forms larger, equant to idioblastic porphyroblasts, known colloquially as buckshot texture.

As well as annealing textures, pyrite has a number of both brittle and ductile deformation textures. Zones of intense cataclasis have resulted in the formation of aggregates of angular comminuted grains. Within these zones a foliation, defined by micas and aligned quartz, anastomose around pyrite porphyroblasts. Locally, thin cataclastic zones marked by concentration of comminuted pyrite and aligned micas, cut across the larger cataclastic zones at a shallow angle. These may be Reidel fractures. Indentation of large porphyroblasts and axial cracking occurs in areas with a high quartz content (Fig. 10).

One sample from the massive pyrite lithofacies looked at in this study shows an excellent example of grain shape preferred orientation of pyrite (Fig. 11). Drill core evidence suggest this sample comes from the overturned limb of a macroscopic fold These elongate grains typically show little or no evidence of brittle deformation, and only minor dislocation microstructure. Grain boundaries are straight to slightly curved, mildly sutured, and lightly indented. No overgrowths are apparent. Preliminary element mapping using a scanning electron microscope suggests growth zoning, outlined by varying intensities of S, Fe, Ni, and As, perpindicular to the long axes of grains (Fig. 12). The growth zoning is truncated, indicating pressure solution is likely the mechanism responsible for formation of the shape preferred orientation.

Pyrite porphyroblasts commonly have overgrowths, either on relict colloform grains or on secondary metamorphic grains. In some cases numerous phases of grain

growth can be recognised in one porphryoblast (Fig. 13). The first phase of growth that can be seen in this example is a hexagonal grain its center. Internal banding in this early phase suggest in may be a relict colloform grain (alternatively it may be an even earlier phase of grain growth). A second phase of growth is suggested by the presence of a straight band of quartz inclusions at a high angle to the earlier and later grain boundaries. This band is interpreted to be a relict grain boundary. Towards the edge of the grain, an inclusion rich area defines yet another phase of grain growth. The grain boundary is defined by the limit of the inclusions. The final phase of grain growth is indicated by the relatively inclusion -free rim around most of the present grain boundary. These multiple phases of grain growth give evidence of a complex history of formation for pyrite in this area. Note also that a well defined foliation in the quartz-rich matrix flows around, and is overgrown by, the pyrite porphyroblast.

Dislocation microstructures

A preliminary examination of dislocation microstructures in pyrite were looked at to determine the deformation mechanisms active in pyrite in the Vangorda deposit. Etched pyrite grains show a number of dislocation microstructures which are characterised by straight to slightly curved, stepped, or branching dislocation walls and tangles (Fig. 14). The dislocation walls and tangles commonly form grid-like arrays denoting the onset of subgrain formation and incipient dynamic recrystallisation.

Subgrain formation is common throughout the samples looked at in this study. Subgrains are typically 5μm - 50μm, equant grains with straight to slightly curved grain boundaries that often meet at 120^{o} triple junctions (Fig. 15). Subgrain formation commonly occurs along the boundaries of parent grains and, as in figure 15, may result in the formation of a core mantle texture, a texture rarely observed in pyrite. Grain boundary bulging (Fig. 16), and incorporation of inclusions into

grains indicate grain growth following subgrain formation.

Conclusions

This report has shown some of the mesoscopic and microscopic characteristics of the deformational style in the ore rocks of the Vangorda. The dominant fabric element found in the deposit is a penetratively developed banding and/or foliation, S_1. S_1 can therefore be used throughout the deposit as a datum marker to reference the relative ages of all structural elements.

S_1 is everywhere folded by tight to isoclinal F_2 folds with a class 2 similiar geometry. In the hinge zones of F_2 folds, S_1 is preserved as lithons, whereas in the fold limbs S_1 has been transposed into parallelism with the F_2 axial surface. In most lithofacies in the deposit an S_2 axial planar cleavage is developed in the hinge areas of F_2 folds. S_2 is typically poorly, or not developed in the more massive pyritic rocks. Qualitatively, F_2 folds have a no ar a small pitch angle in their axial surfaces.

The interference pattern between F_1 and F_2 folds has still not been rigorously defined within the Vangorda deposit. However, the example shown in figure 3 indicates the refolding pattern is likely a type 3 (or hook structure), similiar to that recorded regionally.

Faults in the Vangorda deposit are commonly gouge zones consisting of fine-grained micaceous material or sulphide-quartz sand. However, cemented breccias containing large angular clasts of all ore rocks and phyllites are also found. There are no kinematic indicators in these faults and it is difficult, if not impossible to determine their geometry in drill core.

In the sulphide-rich rocks, however, ductile flow breccias are quite common

and are developed on a scale of centimetres to metres. These faults consist predominantly of pyrrhotite or sphalerite and contain angular to rounded, often tailed clasts of quartz, phyllite, and pyrite. Clasts often have an internal foliation that is not continuous with the external foliation which anastomoses around the clasts. Clasts may be folded, and together with the asymmetry of tails these clasts can be used as kinematic indicators. Ductile flow braccias occur along lithofacies boundaries, indicating layer parallel shearing, and in some instances in the overturned limbs of folds, suggesting concentration of strain in this area of the fold.

Recognition of the geometry of structures on a mesoscopic scale is an important means of determining the structural style of the larger macroscopic folds and faults. With this in mind it is possible to suggest that the macroscopic F_2 fold style in the Vangorda deposit is that of tight to isoclinal, class 3 similiar folds. A S_2 axial planar foliation is developed locally in hinge zones in some, but not all, lithofacies. The dominant planar fabric in the Vangorga deposit is S_1. The fold interference pattern between F_1 and F_2 folds appears to be type 3, the same as that recorded regionally. Recognition of the fold style and the overprinting relationship between folds will allow a more rigorous constraint to be placed on cross sections, long sections, and plan view sections through the deposit. A clear understanding of the style and importance of D_3 to D_5 effects on the Vangorda deposit can only be obtained through careful structural analysis in the open pit.

The relationship between folds and faults is still somewhat ambiguous. Many of the faults clearly truncate the folds, but others appear to be geometrically related to them. This type of problem can only be resolved by rigorous structural analysis in the open pit. It is apparent from this report that it is possible to determine the kinematics of many faults, especially the ductile flow breccias, using a variety of kinematic indicators. This can only be done *in situ* and not in unoriented drill core.

From a microstructural perspective, a number of interesting facts have arisen from preliminary studies of selected, etched samples. Gold, although rare, can be found under a microscope. Sphalerite grains display predominantly annealing textures, and must therefore have undergone significant grain growth following

deformation and recrystallisation. Sphalerite exsolving to chalcopyrite is a reaction that takes place at temperatures of 450 ^{o} C to 500 ^{o} C range, clearly higher than the lower- to mid-greenschist facies temperatures recorded by assemblages in the Vangorda deposit. Fluid composition must, therefore, play an important role in this reaction.

Pyrite displays a number of brittle and ductile deformation textures as well as relict, primary features. Relict colloform grains can still be fund throughout the samples looked at in this study. These may give important clues to the primary nature of the deposit. Brittle features, such as grain indentation and resultant axial cracking are ubiquitous in the Vangorda deposit, indicating that deformation of pyrite occured in the brittle field.

However, numerous textures in pyrite such as preferred grain shape orientation, subgrain formation, pressure solution, and dislocation structures indicated that pyrite was also deforming by ductile mechanisms. Many of the ductile features outline above have been studied experimently (cf. Cox *et al.* 1981) and have be found to occur at temperatures of 500 ^{o}C to 650 ^{o}C and pressures of ~300 MPa, again clearly above the metamorphic conditions indicated by assemblages in the Vangorda deposit. Mechanisms other than pressure and temperature must, therefore, be involved. Fluid composition may play an important role.

Also of interest is the location of the grain shaped preferred orientation in the overturned limb of a macroscopic fold. This would suggest that moe bulk plastic strain occurs in the overturned limb. Not an unreasonable assumption, and may be an important mechanism resulting in faulting along overturned limbs.

AIMS OF FUTURE WORK

Field work during the 1991 field season will concetrate on rigorously defining

the structural style of the Vangorda deposit. Emphasis will be placed on defining the geometry of F_2 folds and the overprinting relations between F_1 and F_2. As well, the geometry and kinematics of faults will be looked at in the pit and the relationships between folds and faults will be defined. The efeect of D_3 to D_5 features will also be looked at closely.

Also, detailed core descriptions will be carried out using existing drill core to better constrain pit data.

A limited amount of regional mapping on the Vangorda Plateau is invisioned for this coming field season. This will provide a more rigorous control on the structural style in the area and thereby place the Vangorda deposit in a more defined structural setting.

Sampling for specific textures and mineralogy will also be done.

The microstructural analysis will continue and be expanded to incorporate mineral assemblages in ore rocks and in shear zones within them. As well, textural studies will be carried out on galena, chalcopyrite, pyrrhotite, sphalerite, and pyrite to determine the active deformation mechanisms in each. Limited chemicial and fluid inclusion analysis will be carried out to determine the conditions of metamorphism.

References

Brown, D. 1990. Structural analysis of the Vangorda open pit mine, Anvil Pb-Zn-Ag District, Faro, Yukon. Report submitted to Curragh Resourses.

Cox, S.F., Etheridge, M.A., Hobbs, B.E. 1981. The experimental deformation of polycrystalline and single crystal pyrite. Economic Geology, v.76, p. 2105-2117.

Jennings, D.S., Jilson, G.A., Pigage, L.C. 1980. Anvil Range stratigraphy, south central Yukon Territory; (pog. with abst.), Cordilleran Section, Geol. Assoc. Can., p.16-17.

Jennings, D.S., and Jilson, G.A. 1987. Geology and sulphide deposits of Anvil Range, Yukon. in Morin, J.A. (ed.) Mineral Deposits of the Northern Cordillera. CIM Special Volume 37, p. 319-361.

Marshall, B. and Gilligan, L.B. 1989. Durchbewegung structure, piercement cusps, and piercement veins in massive sulphide deposits: formation and interpretation. Economic Geology, v.84, p.2311-2319.

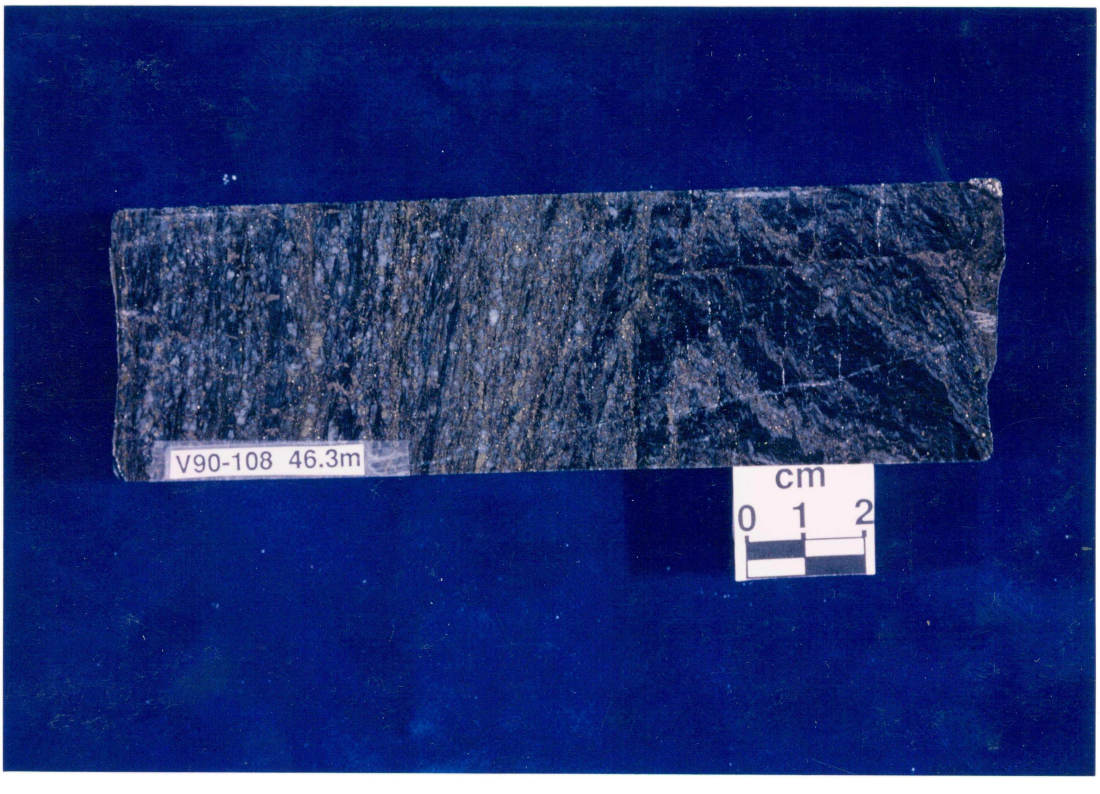

Figure 1. Lithon texture in which S_1 is preserved in the fold hinge of a F_2 fold.

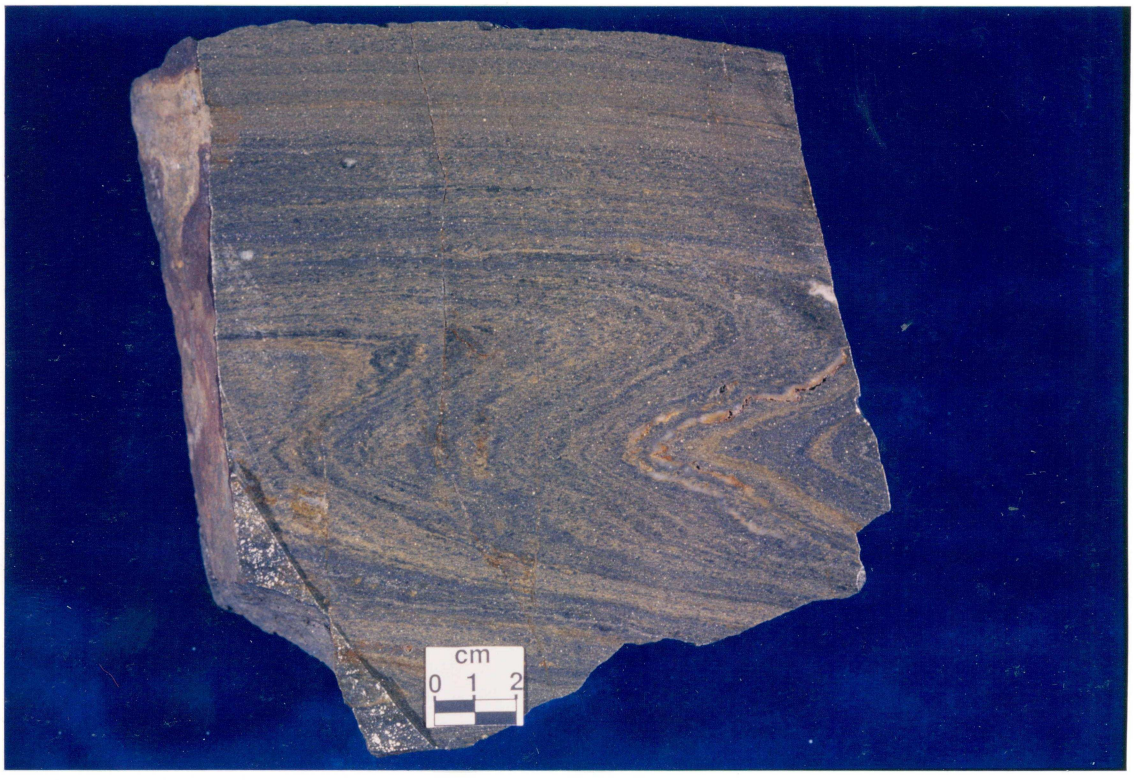

Figure 2. F_2 similiar fold in pyritic quartzite. Note the small interlimb angle and the thickening in the fold hinge.

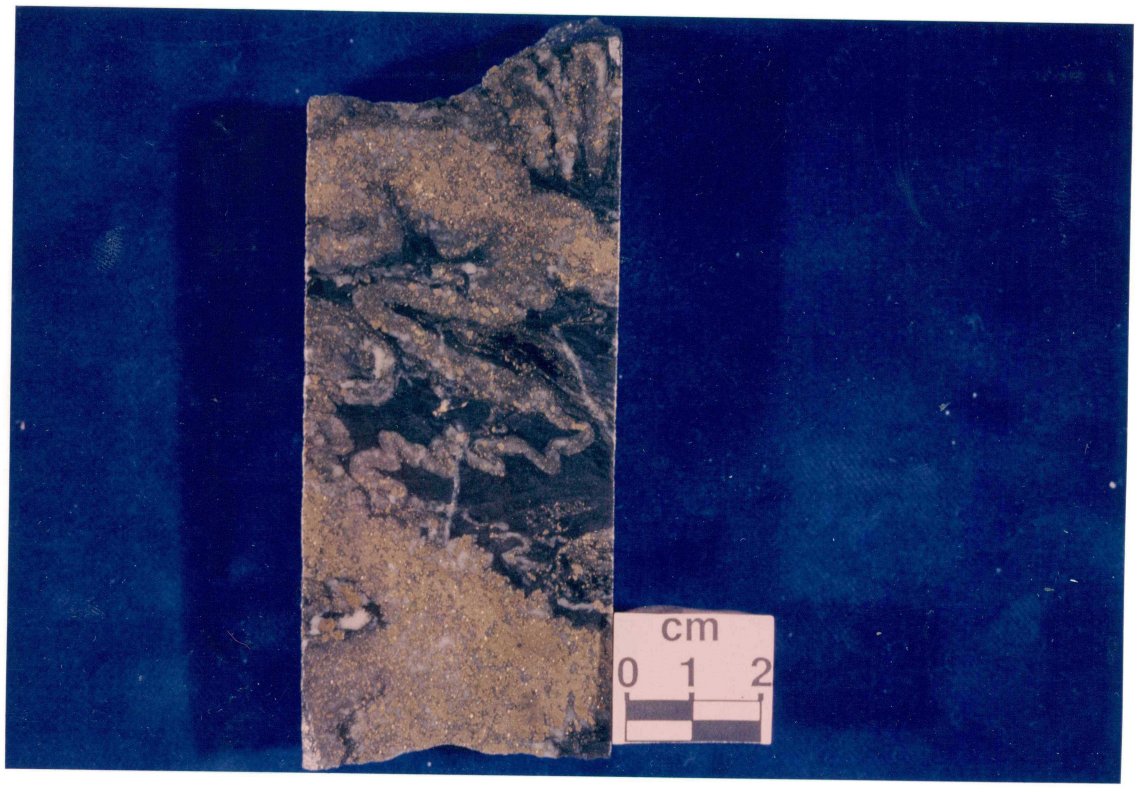

Figure 3a. Tightly F_2 folded quartz band in the ribboned-banded carbonaceous quartzite lithofacies. The S_2 axial surface dips ~ 110^o relative to the core axis.

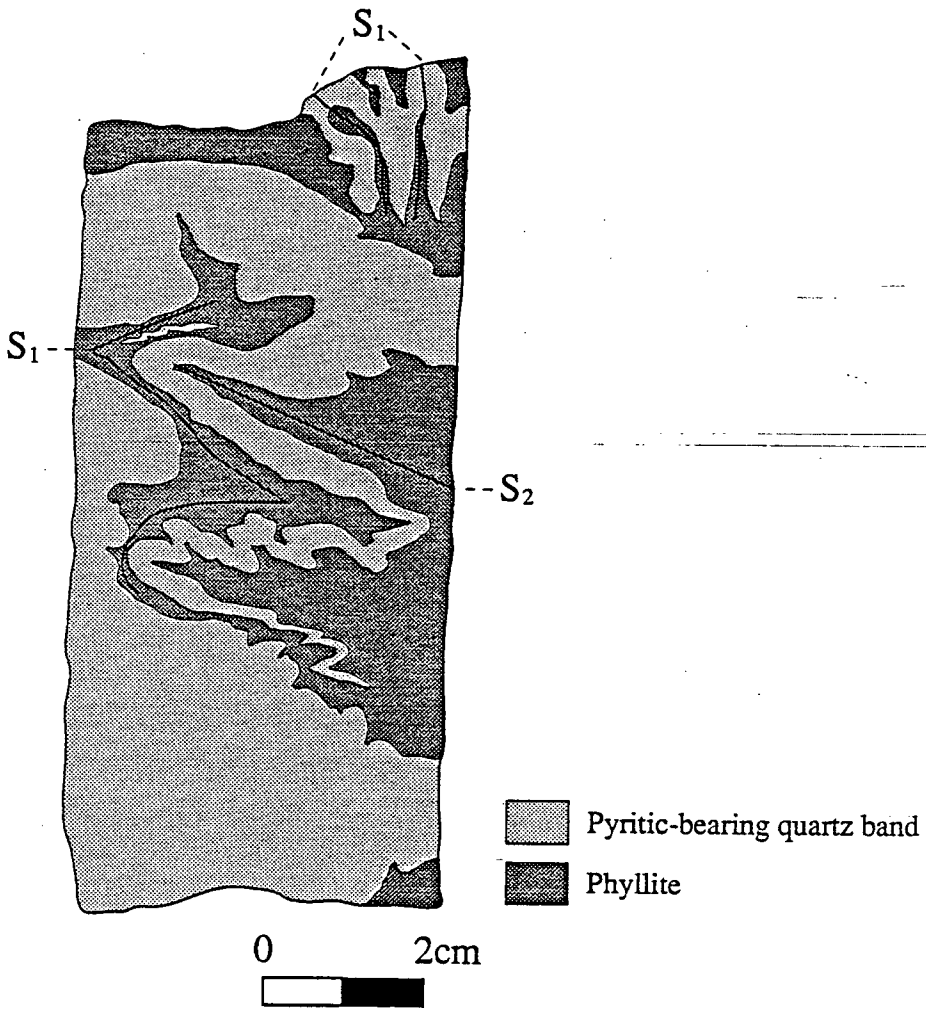

Figure 3b. Schematic interpretative drawing of figure 3a showing the orientation and location of the different structural elements. The refold pattern indicated by the S1 axial trace is type 3.

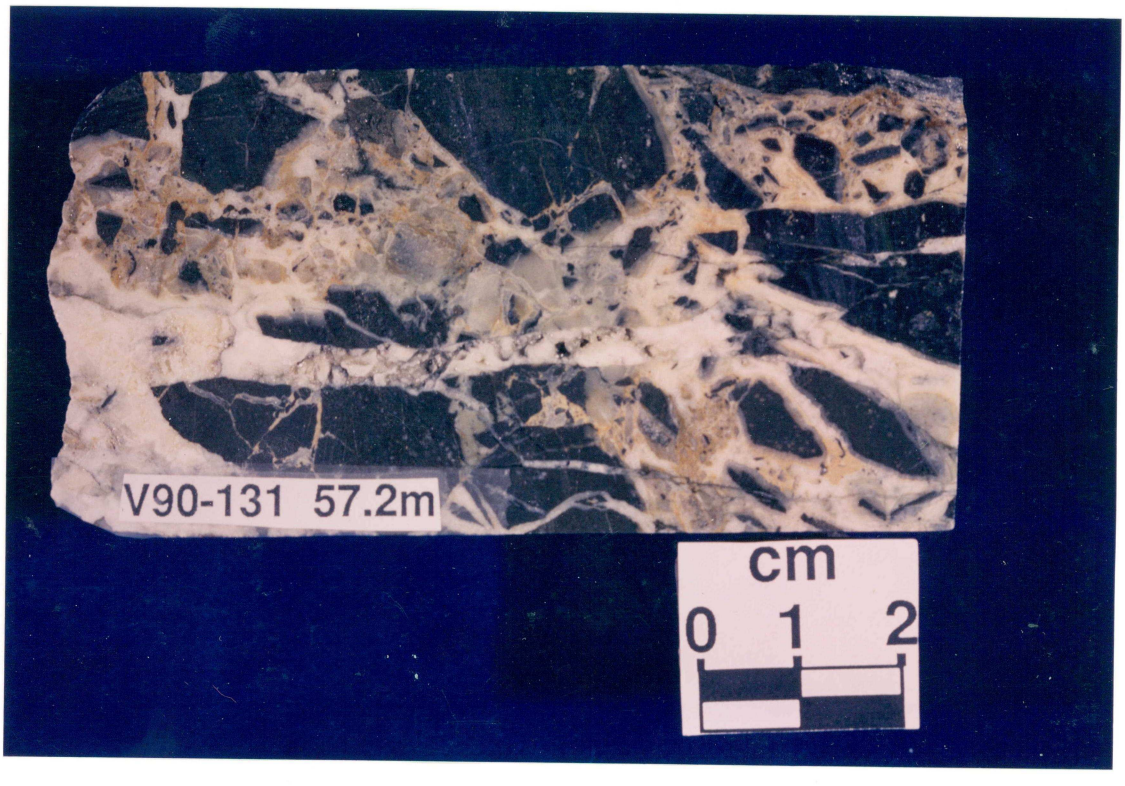

Figure 4. Well cemented brittle fault in a massive sulphide. The matrix consists of quartz and carbonate. Clasts are massive sulphide and quartz. The presence of angular quartz clasts suggest a previous phase of fault cement that was subsequently brecciated by the present movement episode. Note the clear quartz overgrowths on all clasts

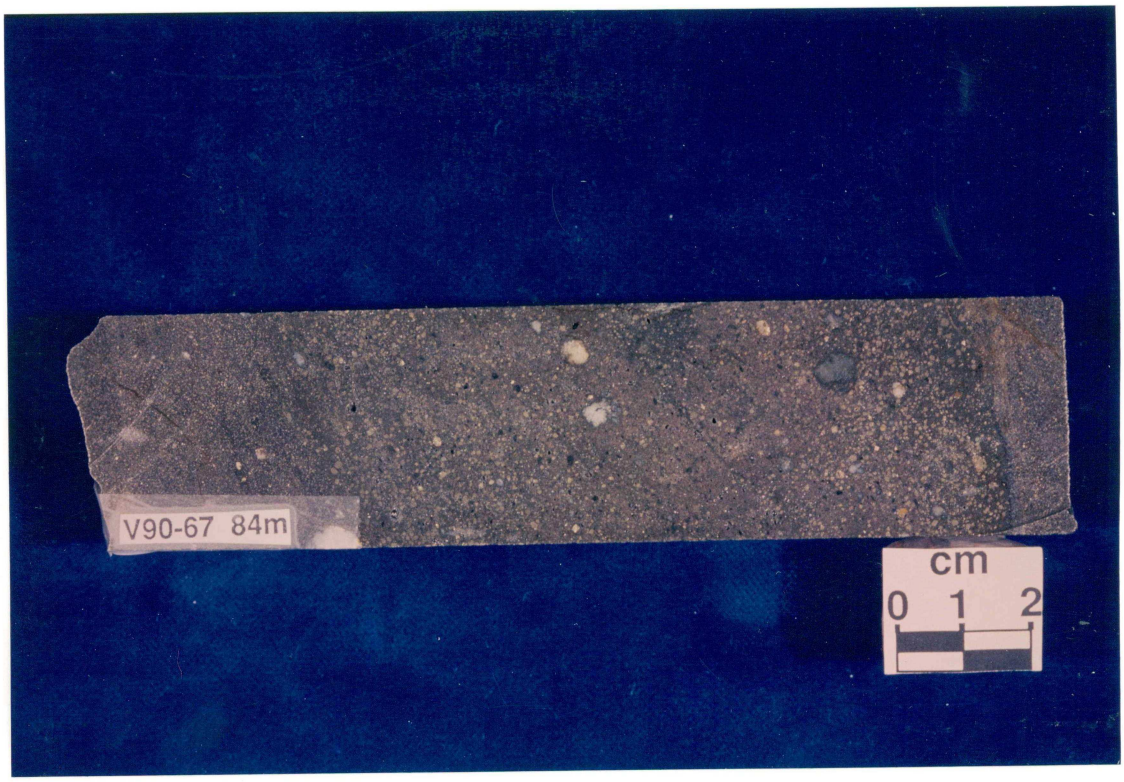

Figure 5. Ductile flow breccia containing well rounded, equant clasts of quartz (white), phyllite (dark grey), and sulphide (bronze). A foliation in the fault dips steeply relative to the core axis. Note the knife sharp boundary oriented subperpindicular to core axis. Note also the ubiquitous presence of sub-millimetre porphyroblasts of pyrite in the fault zone.

Figure 6a. Tightly F2 folded (note the presence of a folded foliation within the band) and brecciated pyrite band in a flowing matrix of sphalerite massive sulphide lithofacies. Note tailed pyritic clasts near the bottom.

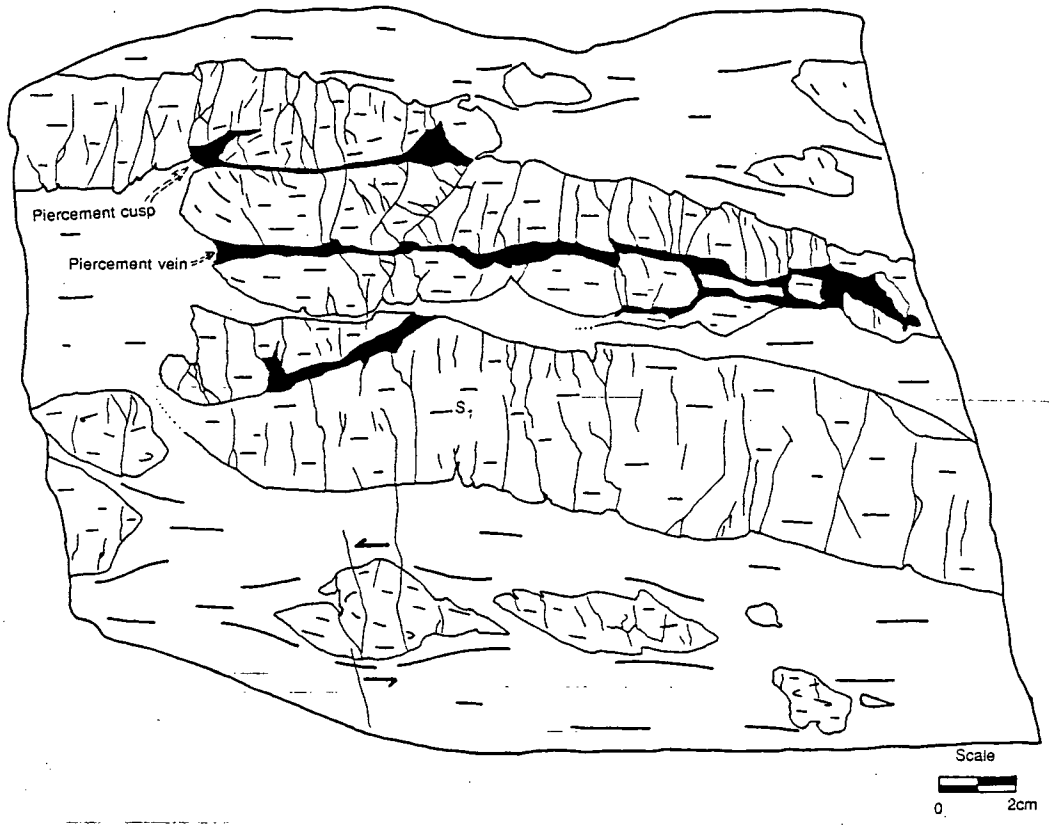

Figure 6b. Interpretive shetch of figure 6a. Piercement cusps and veins (black) penetrate the folded pyrite band causing it to boudinage and brecciate. The tailed clasts near the bottom have a tightly folded internal foliation that, together with the asymmetry of the tails, give a shear direction.

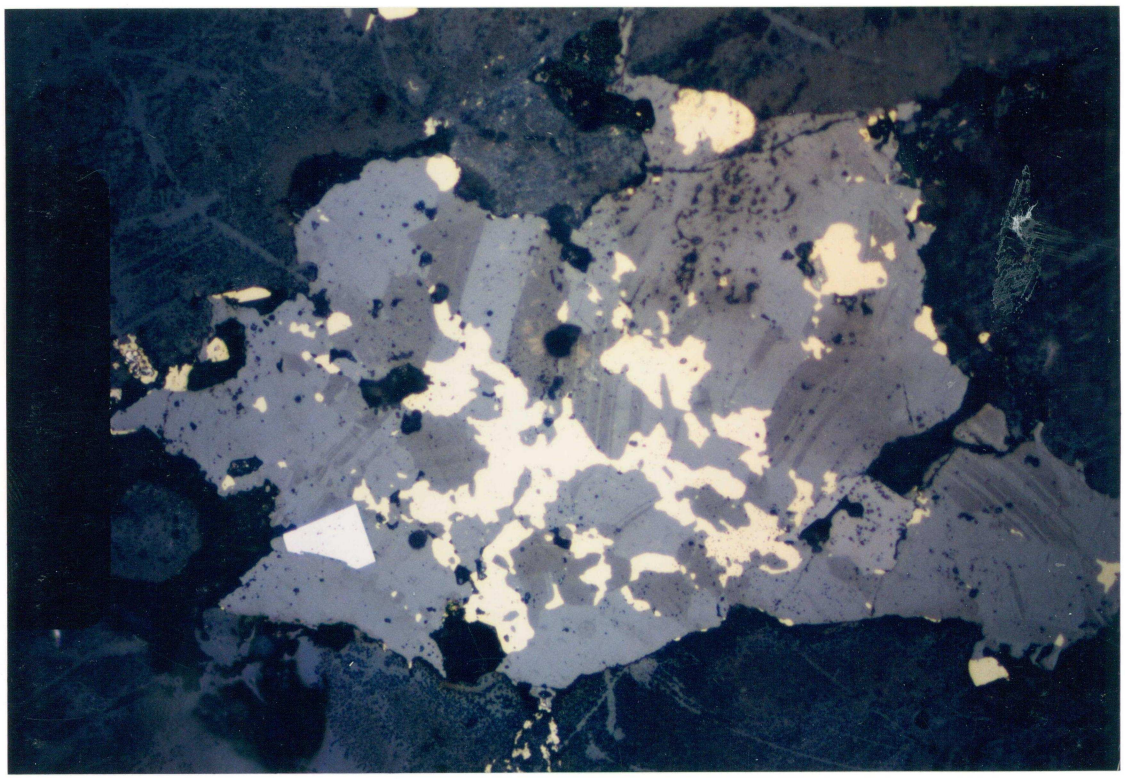

Figure 7. Aggregate of sphalerite grains (light grey) with broad annealing twins. Grain boundaries did not etch well in this example. Sphalerite is exsolving to chalcopyrite (bright yellow) which truncates the twins. The bright cubic grain is arsenopyrite. Magnification is 20x.

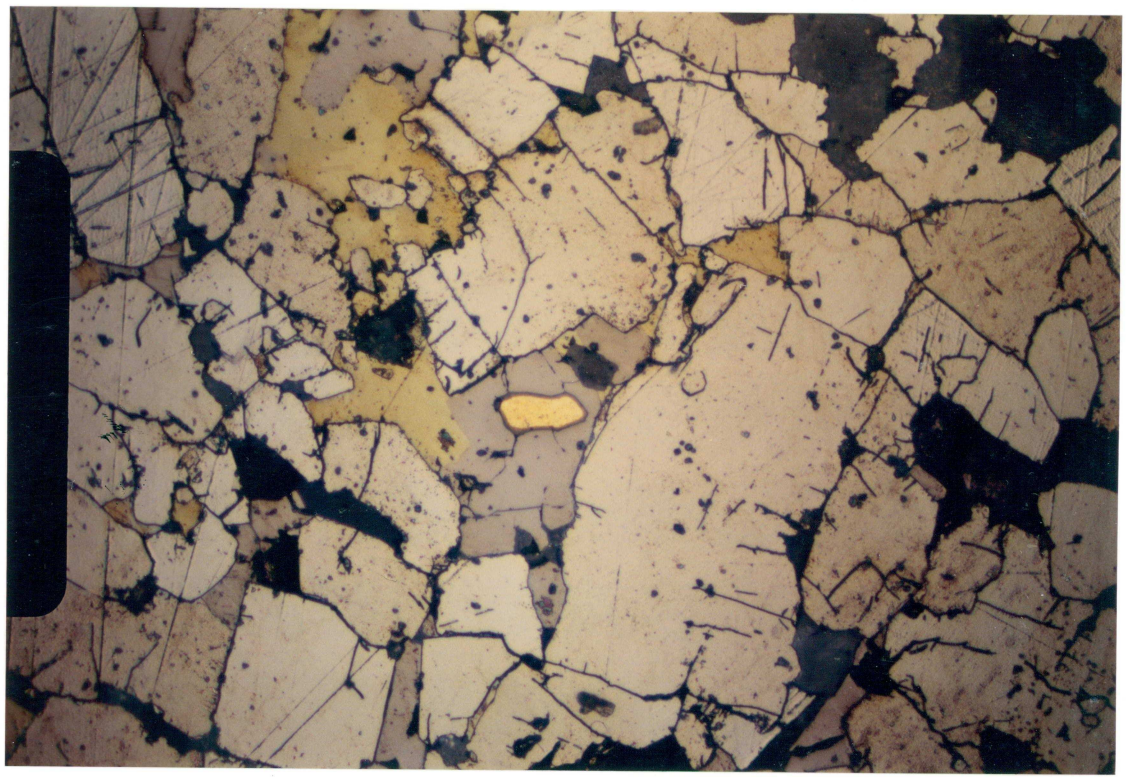

Figure 8. Grain of gold (gold color) as an inclusion in pyrrhotite (pinkish) in the spaces between larger pyrite porphyroblasts (brass color). Magnification is 20x.

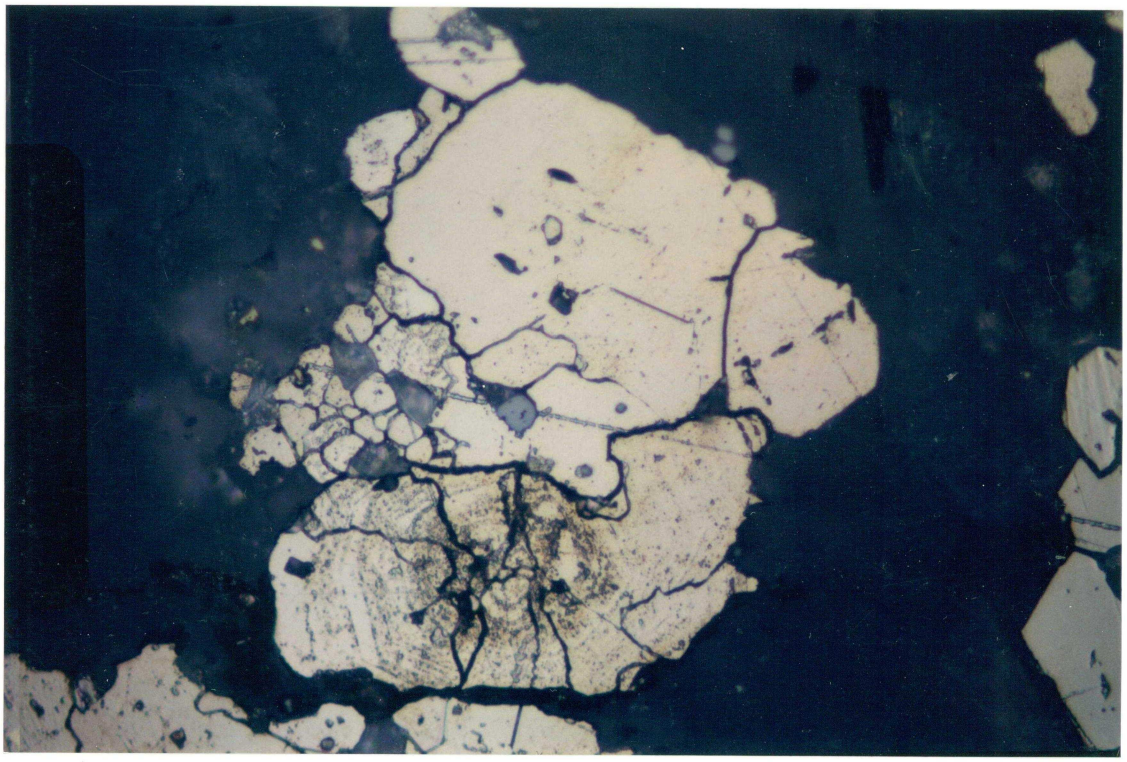

Figure 9. Relict, primary colloform pyrite being indented by secondary metamorphic pyrite. The colloform grain displays pressure solution along its boundary with the metamorphic grain, and has undergone significant cracking. Magnification is 40x.

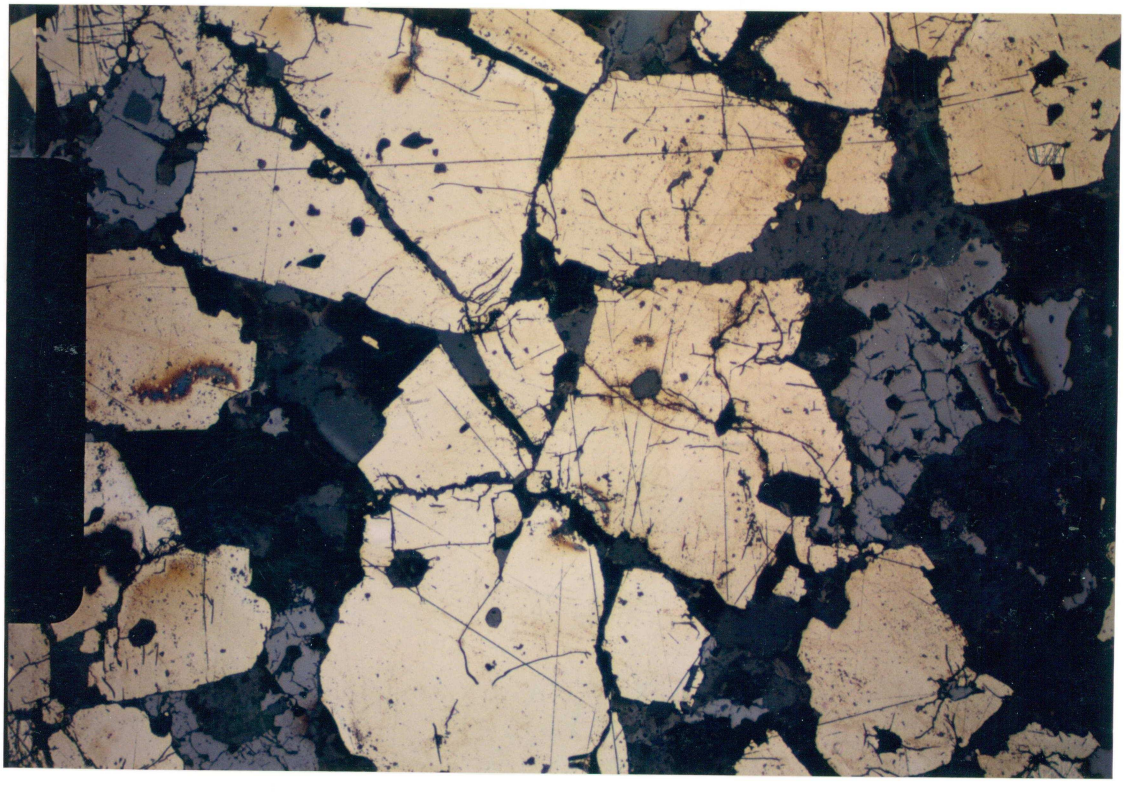

Figure 10. Porphyroblasts of pyrite showning indentation and axial cracking. Note the increase in crack frequency in the area of indentor contact. Magnification is 10x.

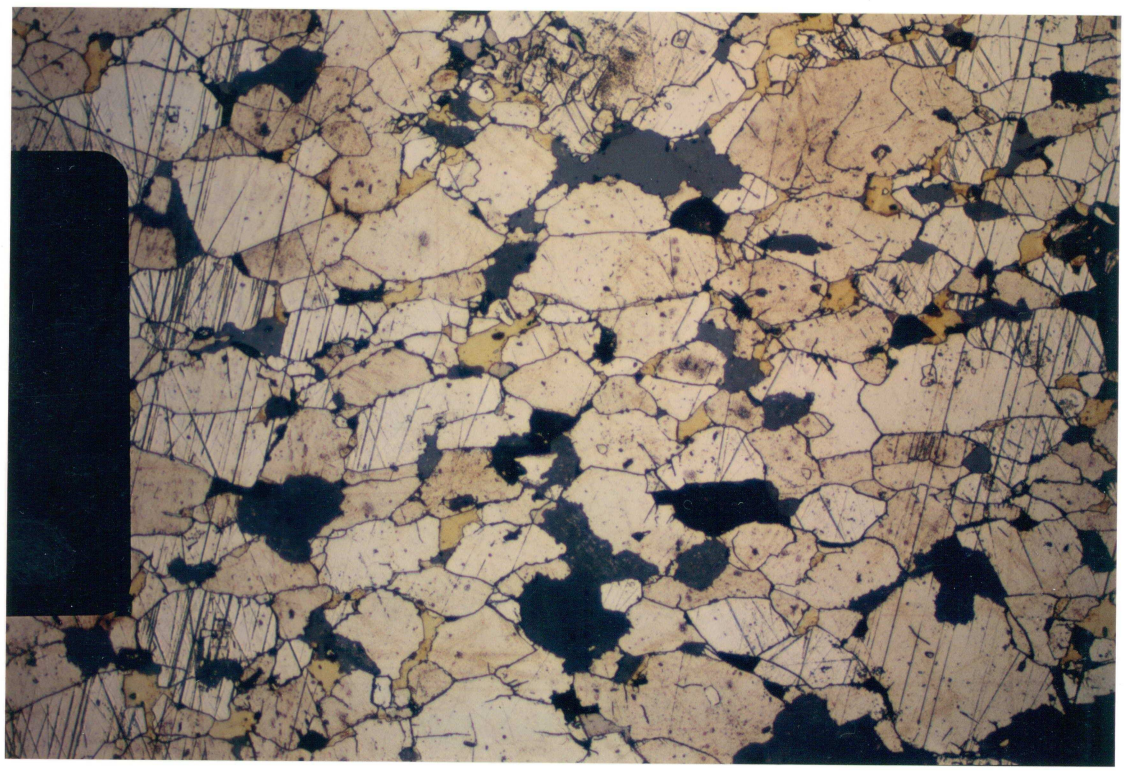

Figure 11. Well developed grain shape preferred orientation in pyrite. Grain boundaries are typically straight to slightly curved. Chalcopyrite (brass colored) infill the spaces between the pyrite grains. Magnification is 10x.

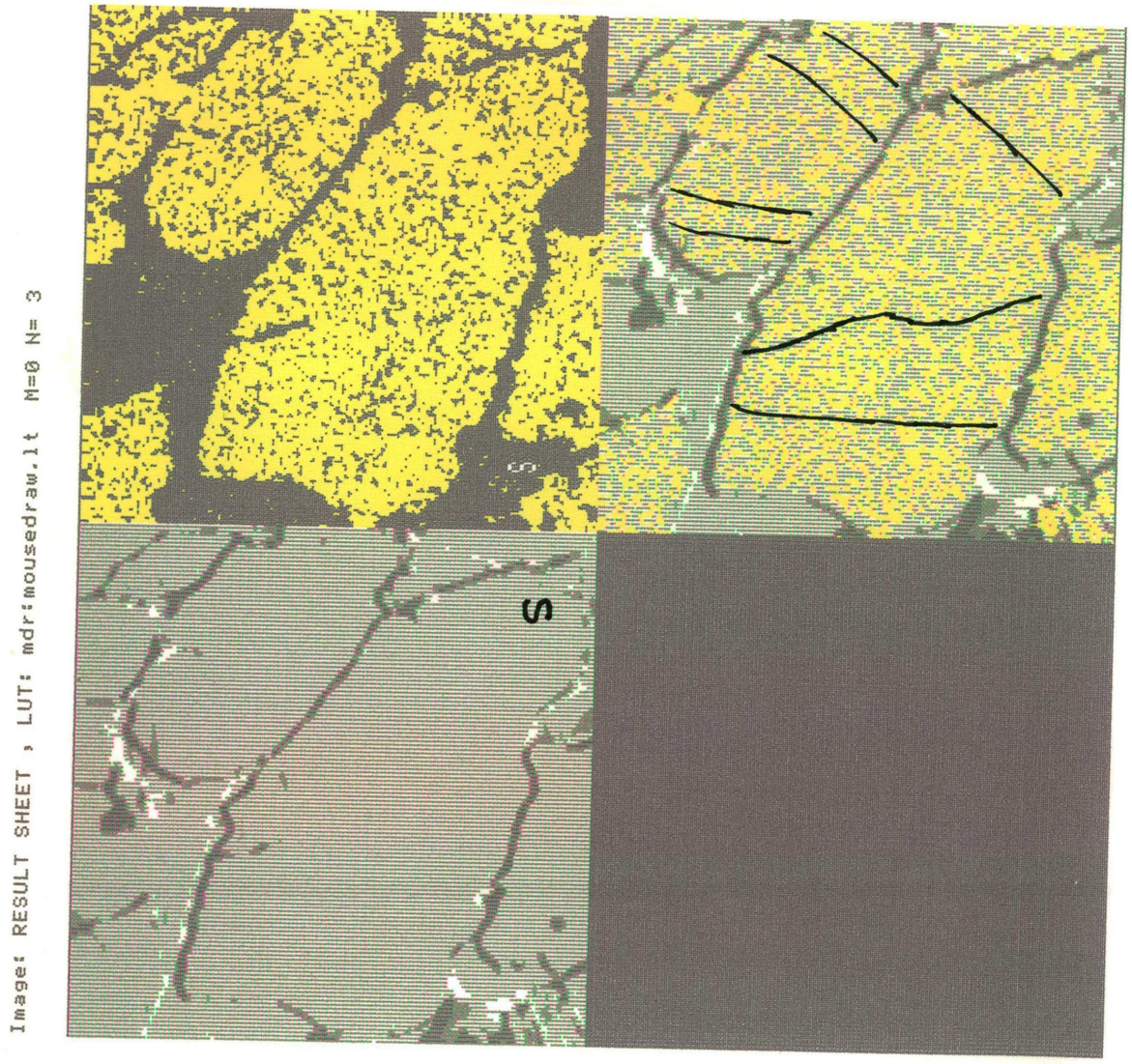

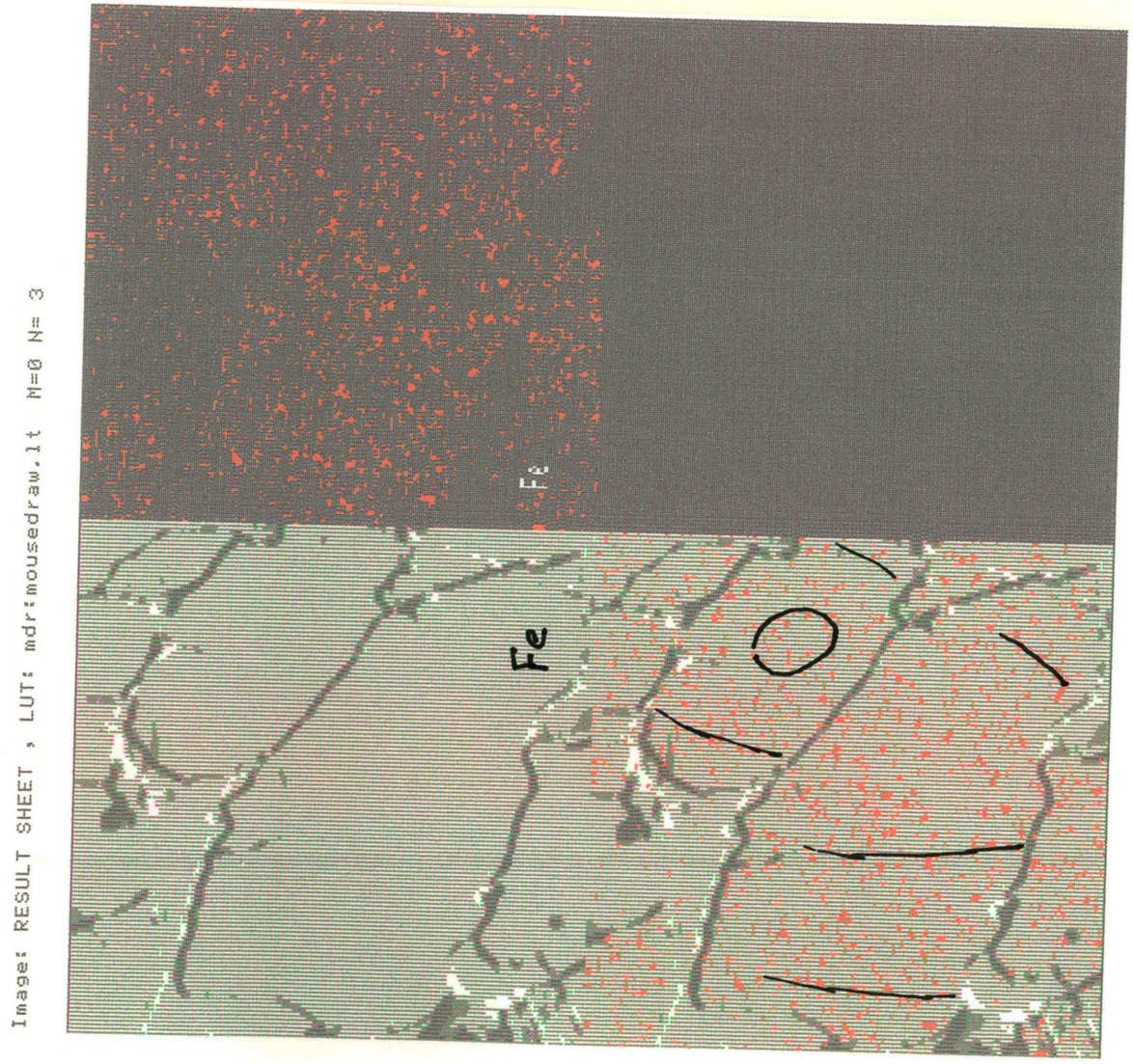

Figure 12. Scanning electron microscope map of elongate pyrite grains. Growth zones, shown by interpretative lines, are truncated by grain boundaries. The interpretation is made possible by the much better resolution of the SEM computer screen.

Image: RESULT SHEET , LUT: mdr:mousedraw.lt M=0 N= 3

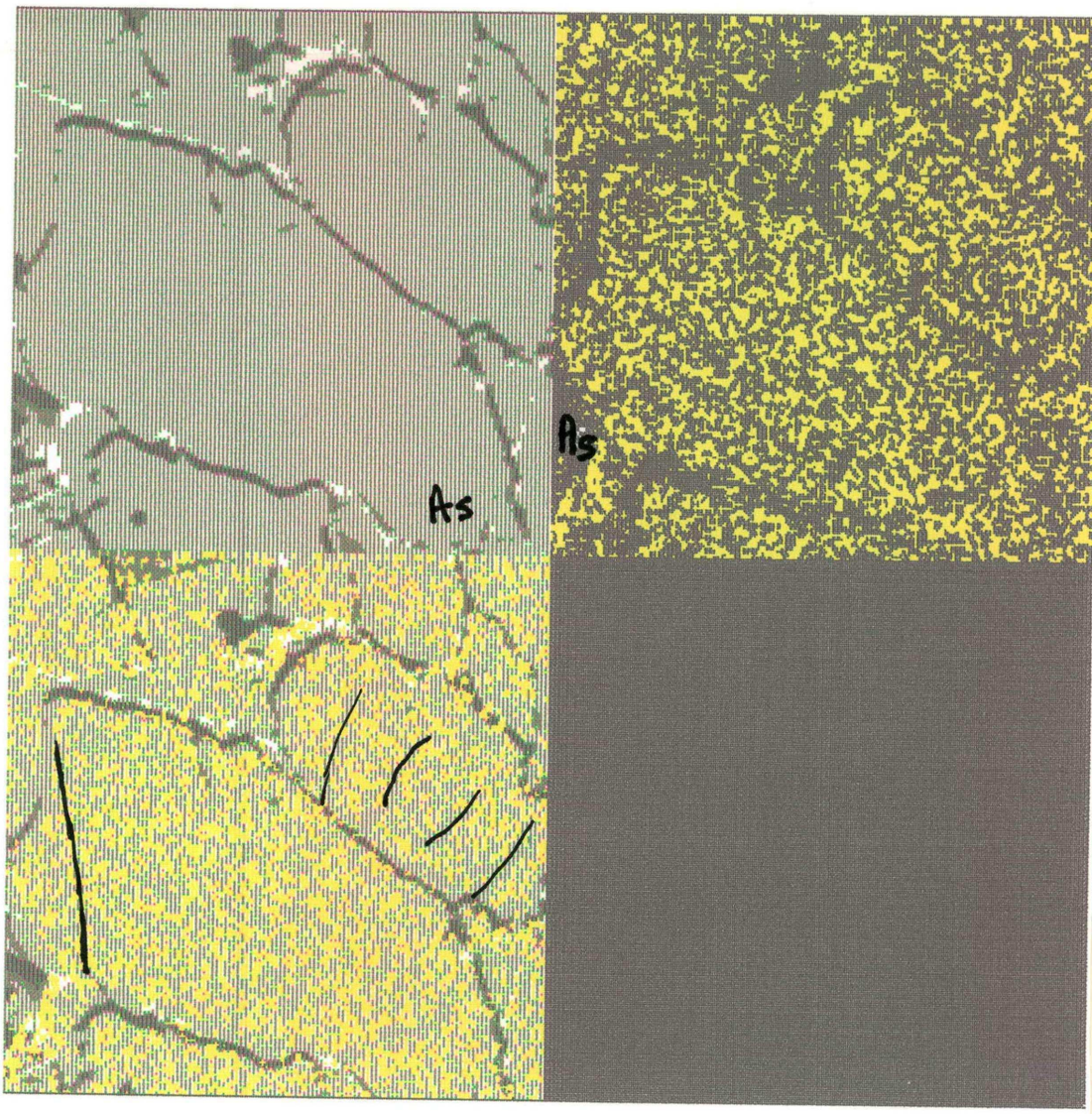

Image: RESULT SHEET , LUT: mdr:mousedraw.lt M=0 N= 3

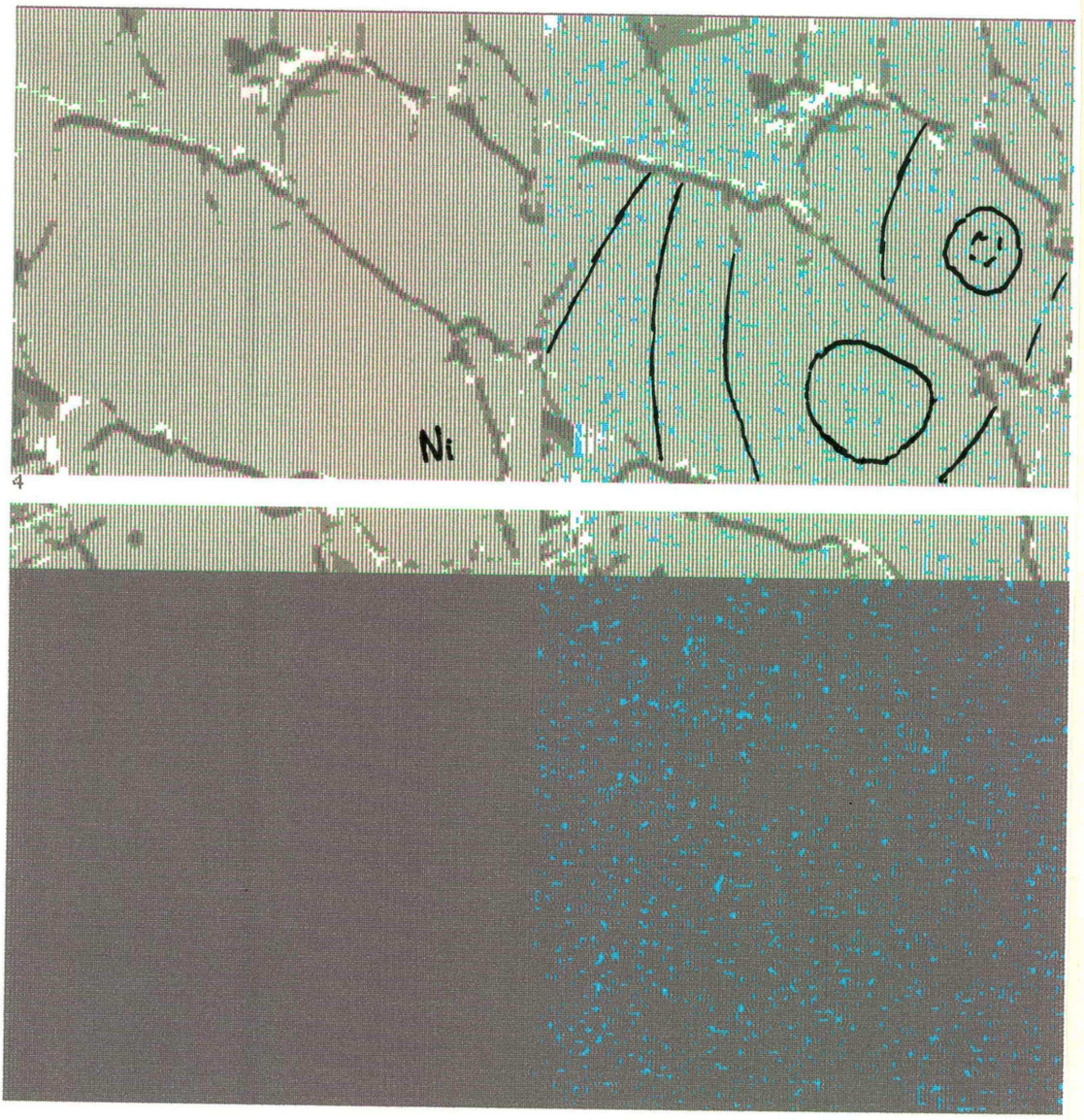

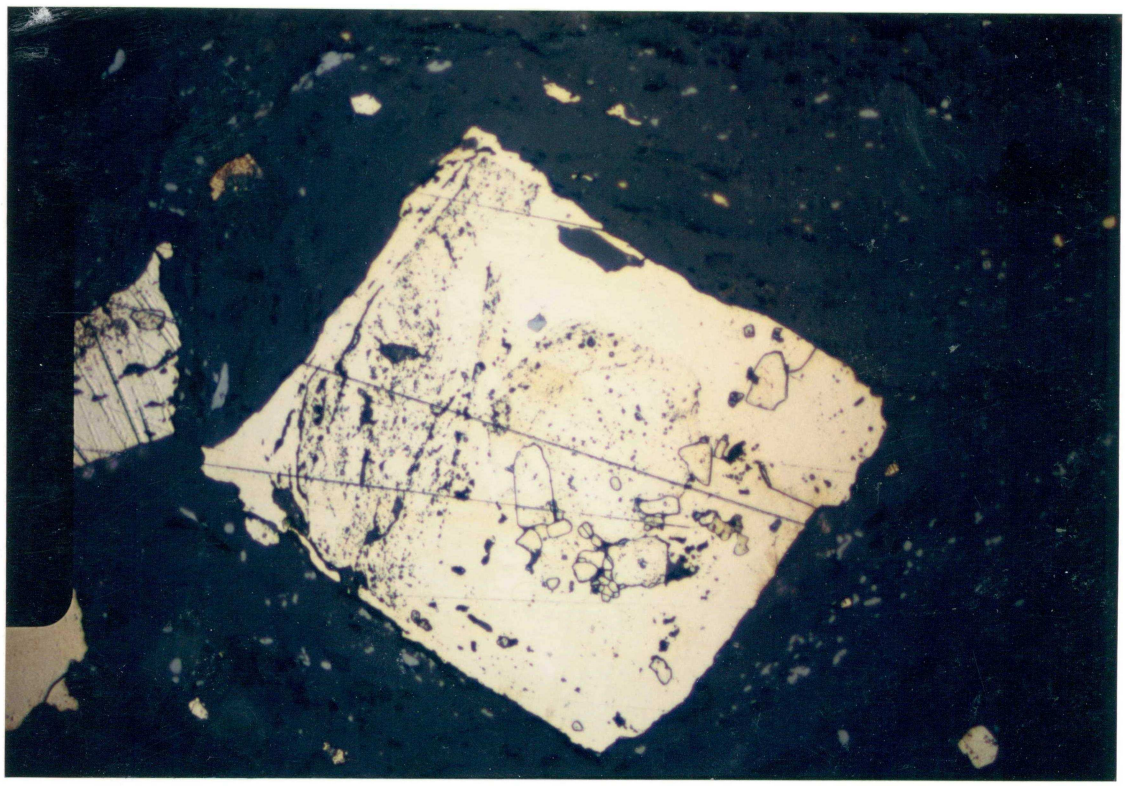

Figure 13. Pyrite porphyroblast with numerous overgrowths (see text for further discussion). The matrix, defined by quartz and mica, wraps around the porphyroblast. Magnification is 20x.

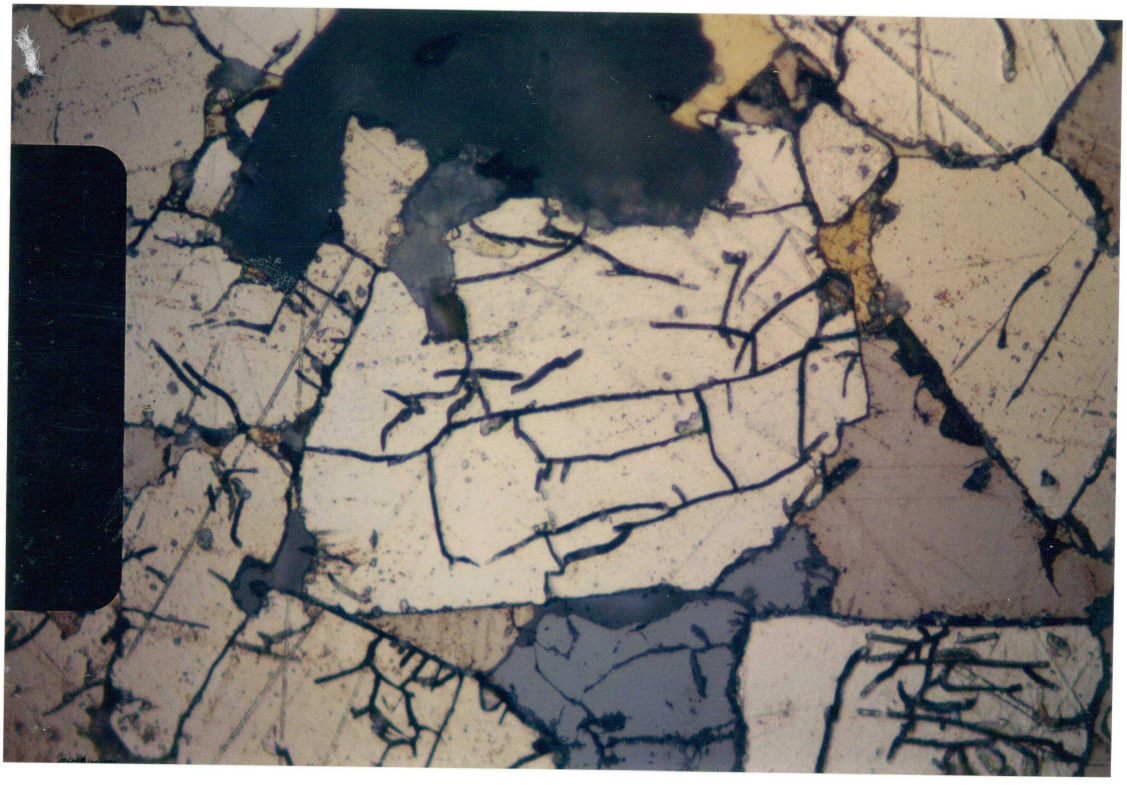

Figure 14. Dislocation walls and tangles in pyrite showing incipient formation of elongate and equant subgrains. Magnification is 40x.

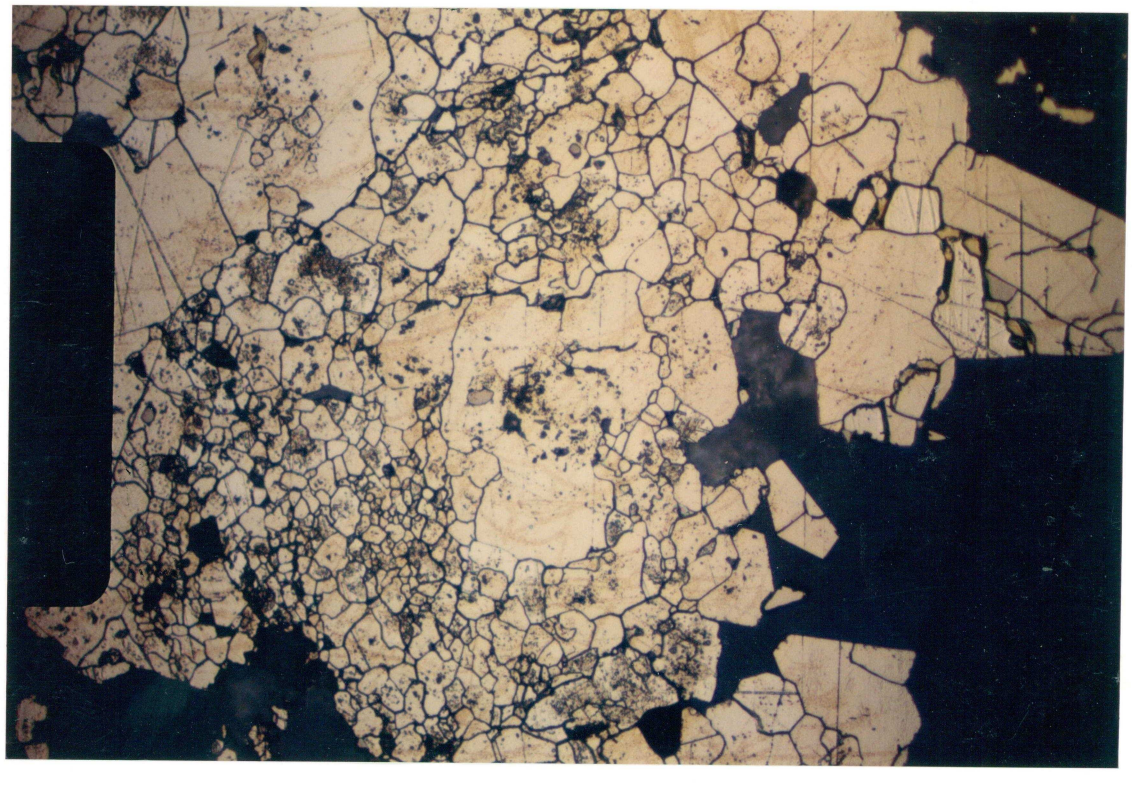

Figure 15. Equant subgrains around a relict core forming core and mantle texture. Subgrain boundaries are straight and meet at 120^{o} triple junctions. Inclusions in the core may form an helicitic inclusion pattern. Magnification is 20x.

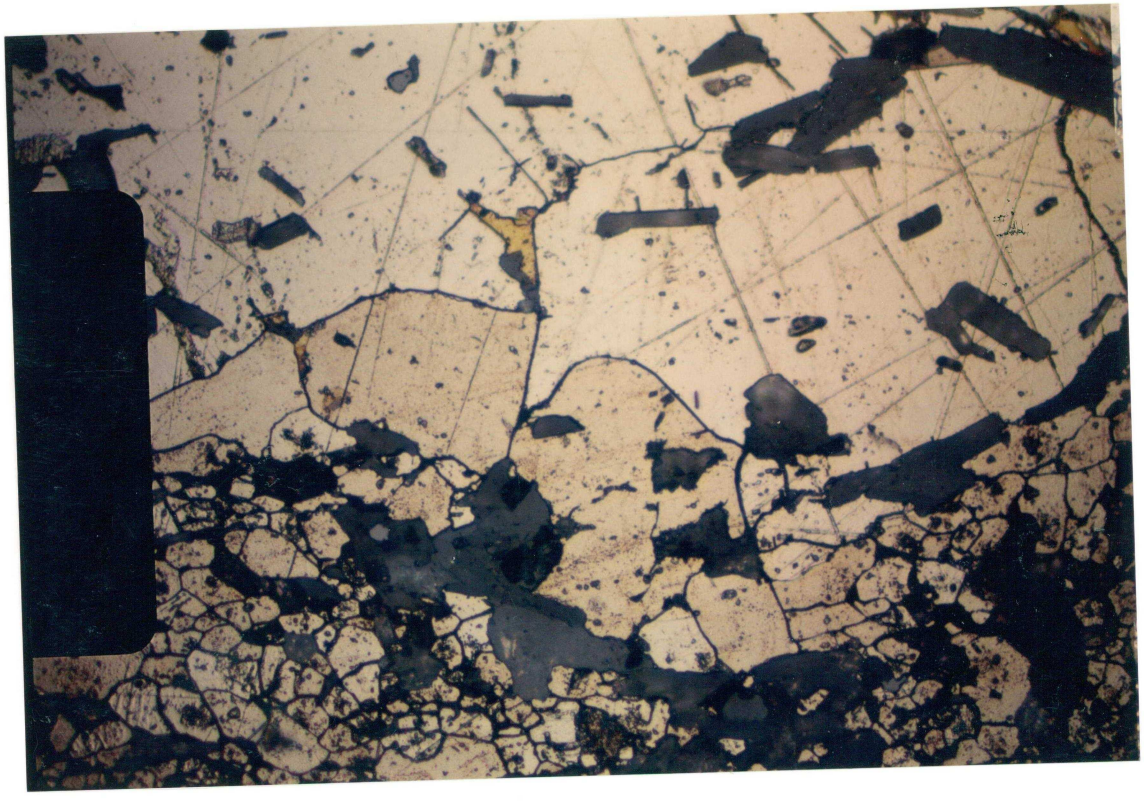

Figure 16. Lobate grain boundaries in pyrite indicating grain boundary migration by bulging. Magnification is 10x.